

# Use of the successive self-nucleation and annealing technique to characterize $^{60}\text{Co}$ gamma irradiated HDPEs

Blanca Rojas de Gás cue · José Luis Prin ·  
Gilma Hernández · Enrique M. Vallés ·  
Arnaldo T. Lorenzo · Alejandro J. Müller

Received: 3 April 2010/Accepted: 20 October 2010/Published online: 3 November 2010  
© Akadémiai Kiadó, Budapest, Hungary 2010

**Abstract** The application of the Successive Self-nucleation and Annealing (SSA) thermal fractionation technique can yield detailed information of the structural changes induced in linear polyethylene by irradiation. The production of tertiary carbons during the crosslinking reactions can be equivalent to the structural heterogeneity present in branched polyethylenes since in both cases interruption of the linear crystallizable sequences occurs, and these are structural differences that can be easily detected by thermal fractionation. We demonstrate how correlations between melting point and short chain branching content employed for branched polymers can be useful to characterize the distribution of chain heterogeneity produced by crosslinking. As the radiation dose is increased and the crosslinking content also increases, the distribution of chain heterogeneity gets broader as detected by SSA. When the results are coupled with morphological observations made by transmission electron microscopy, valuable information on the morphological changes produced by crosslinking can also be ascertained, since the distribution of lamellar thicknesses substantially broadens

with crosslinking. Such a broad distribution can also be predicted from SSA by simple calculations performed employing a modified version of the Gibbs–Thomson equation and is expected on the basis of random cross-linking reactions.

**Keywords** SSA · HDPE · Thermal-fractionation

## Introduction

Polyethylene (PE) is still the largest commodity polymer produced worldwide. However, the need to develop new PE grades with improved physical and chemical properties has been always a challenge; hence, research on this polyolefin is still challenging. In this sense, the controlled crosslinking of PE by irradiation [1–3] or by the addition of peroxides [4–13], has been reported as a way to improve the thermal and mechanical properties of the material. Crosslinked polyethylenes (PEs) could have similar thermo-mechanical properties as more expensive engineering polymer materials such as nylons.

The irradiation of PEs with high-energy ionization can be used to modify properties such as the tensile strength and stress cracking resistance. However, the increase in the thermo-mechanical properties will depend on the knowledge of the relationship between radiation dose and the structural changes induced on the samples. It has been reported that in irradiated or chemically modified linear PEs, crosslinking reactions will predominate, favoring the creation of reticulated material (high content of crosslinked material) [3–7]. As the content of crosslinked chains increases in PEs, the tensile modulus tends to increase the yield strength as well, while the elongation at break is reduced [14]. Any interruption of the linear crystallizable

B. R. de Gás cue (✉) · J. L. Prin · G. Hernández  
Instituto de Investigaciones en Biomedicina y Ciencias Aplicadas, IIBCA-UDO, Universidad de Oriente, Cerro del Medio, Núcleo de Sucre, Cumaná, Edo. Sucre, Venezuela  
e-mail: blanca\_gascue@yahoo.com

E. M. Vallés  
Planta Piloto de Ingeniería Química, PLAPIQUI (UNS-CONICET), Camino La Carrindanga Km 7 - (8000), Bahía Blanca, Argentina

A. T. Lorenzo · A. J. Müller  
Grupo de Polímeros USB, Departamento de Ciencia de los Materiales, Universidad Simón Bolívar, Apdo. 89000, Caracas 1080-A, Venezuela

sequences of PE chains (both by branching or crosslinking) will affect their crystallization properties and the maximum lamellar sizes attained.

Successive Self-nucleation and Annealing (SSA) is a thermal fractionation technique, developed by Müller et al. in 1997, which has gained wide acceptance in the literature [15–19]. It is based on the sequential application of self-nucleation and annealing steps to a polymer sample in decreasing temperature steps in a Differential Scanning Calorimeter (DSC). After thermal conditioning, a final heating run reveals the distribution of melting points induced by the SSA treatment as a result of the heterogeneous nature of the chain structure of the polymer under analysis. SSA is performed at substantially shorter times than other thermal fractionation protocols (like step crystallization and temperature rising elution fractionation) and with better resolution [15–19]. A detailed comparison of the different thermal fractionation techniques can be found in reference 17 (and references there in). The nature of the polymer chain must, therefore, be heterogeneous in order to have a wide distribution of crystallizable chain segments, such as in random ethylene/ $\alpha$ -olefin copolymers, crosslinked PEs or polymers with tacticity defects that interrupt crystallizable sequences or random-copolymers. These are the best candidates for thermal fractionation [17, 20, 21] SSA as many other thermal fractionation techniques do not produce fractionation based on molecular mass differences [17].

The SSA technique has been previously employed to assess changes in the molecular structure of polyethylene chains when they are crosslinked. The first study that reports the application of SSA to crosslinked PE was that of Paolini et al. [22]. Paolini et al. studied the thermal behavior of crosslinked low density polyethylene (XLPE) employed as an insulator for commercial underground high tension (15 kV) cables. Three types of materials were used by Paolini et al.: an uncrosslinked low density polyethylene (NXLPE), an XLPE, and an aged XLPE sample. The aging conditions involved the application of multiple stresses: temperature, voltage, and voltage impulses during 60 days. The effect of thermal fractionation under multiple stresses conditions was analyzed by measuring the percentage of crosslinking before and after the aging tests were performed, and by investigating the thermal response of the material by conventional DSC and by the application of SSA. The degree of crosslinking was found to vary in the material depending on the distance from the conductor because a thermal gradient was generated radially during the curing reaction. Such differences did not significantly affect the standard DSC heating scans of the samples. However, when SSA was applied, a difference in the distribution of thermal fractions was detected as a function of the distance toward the conductor that could be correlated

to the variations in the crosslinking degree. After the accelerated aging the thermal response of XLPE changed as evidenced by the presence of multiple melting peaks in subsequent DSC heating scans. This multiple melting arose from thermal fractionation during aging, and SSA was able to simulate a similar fractionation that was very accurate in the prediction of the exact temperatures of the melting peaks produced.

Recently, Pérez et al. [7] have applied SSA to study the peroxide crosslinking of hydrogenated polybutadiene samples which represent model linear low density polyethylenes (LLDPE, equivalent to ethylene-butene copolymers). They employed four LLDPEs of different molecular masses modified with several concentrations of 2,5-dimethyl-2,5 di(tert-butyl peroxy)-hexane (DBPH) as a crosslinking initiator. The crosslinking reaction affected the semicrystalline structure of the materials, and the changes were followed by SSA. They concluded that the variations in the lamellar thickness distributions of the material were related to the peroxide induced free radical reactions.

In this study, SSA is applied to high density polyethylene (HDPE) irradiated with different doses of gamma radiation, aiming to establish a relationship between the radiation dose and the structural changes of the HDPE linear chains. These changes were also verified using transmission electron microscopy (TEM) and performing a comparison between experimental versus theoretical (apparent) lamellar thickness distributions.

## Experimental section

### Material

A high density polyethylene with a number and mass average molecular mass of 19 and 54 kg mol<sup>-1</sup>, respectively, was employed.

### Irradiation protocol

The HDPE samples were irradiated with a <sup>60</sup>Co gamma radiation energy source, at the Atomic Energy National Commission of Argentina. The experimental protocol used in this study has been reported elsewhere [2, 4], and can be summarized as follows:

### Vacuum packing

Rectangles of HDPE (0.5 × 4 × 12 mm) were cut from compression molded HDPE sheets, and were placed inside glass ampules; the glass ampules were sealed under high vacuum conditions (10<sup>4</sup> torr) for two continuous days.

### Irradiation

The samples were exposed to  $^{60}\text{Co}$  gamma source. The used dose rate was  $3.3 \text{ kGy h}^{-1}$ . Three total doses were attained (70, 100, and 200 kGy) and applied to each sample. After irradiation, the samples were stored under vacuum and at room temperature for 1 week.

The samples were characterized after a 4-h annealing at  $150^\circ\text{C}$  (the annealing was performed using the same vacuum packing employed for the irradiation procedure), which was performed in order to eliminate the radicals originated from the irradiation process.

### Gel fraction

The irradiated HDPE samples were heated at  $140^\circ\text{C}$  in 1,2,4-trichlorobenzene (1,2,4-TCB), in order to separate the gel fraction (totally insoluble) from the soluble fraction, both present within the HDPE samples.

### Standard thermal analysis

The standard thermal analysis of the samples was performed in a Perkin-Elmer Differential Scanning Calorimeter (DSC7) under high-purity nitrogen atmosphere and calibrated using Indium and Tin standards. The samples were evaluated as small disks of approximately 10 mg in mass. The standard thermal protocol employed was: (a) a heating run from room temperature to  $170^\circ\text{C}$ ; (b) holding the samples at  $170^\circ\text{C}$  for a 3-min period, in order to erase all the previous crystalline history; (c) the samples were controlled cooled from the molten state down to  $25^\circ\text{C}$  at  $10^\circ\text{C min}^{-1}$ ; (d) after a 3-min holding time at  $25^\circ\text{C}$ , the samples were heated up to  $170^\circ\text{C}$  at  $10^\circ\text{C min}^{-1}$  to record the second heating run.

### Successive self-nucleation and annealing (SSA) thermal fractionation technique

In the SSA protocol [15–19] the following steps are performed (see Fig. 1 for a graphic explanation):

- The sample is held in the melt at  $170^\circ\text{C}$  for 3 min to erase thermal history.
- The sample is cooled, at a constant rate of  $10^\circ\text{C min}^{-1}$ , to a lower temperature limit ( $25^\circ\text{C}$ ) in order to allow the crystallization of the material. The peak crystallization temperature recorded during this cooling scan will be referred to as the “standard” crystallization temperature (or standard  $T_c$ ).
- Self-nucleation step (or self-nucleation and annealing) [23]. The sample is heated at  $10^\circ\text{C min}^{-1}$  from  $25^\circ\text{C}$  to a selected self-seeding temperature (that we shall term  $T_s$ ).

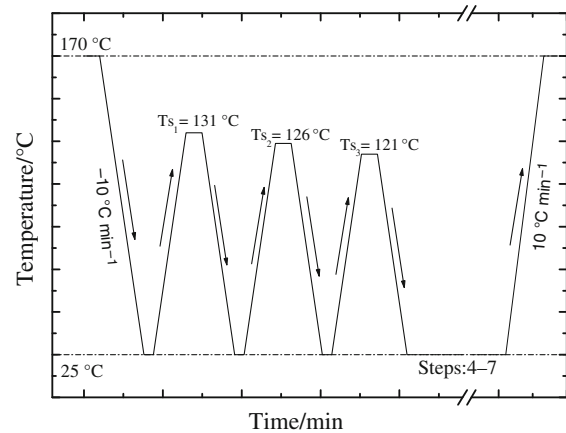


**Fig. 1** Illustration of the SSA thermal protocol applied to all samples

- The sample is held at this  $T_s$  for 5 min. This isothermal treatment at  $T_s$  results in partial melting and, depending on  $T_s$ , in the annealing of unmelted crystals, while some of the melted species may isothermally crystallize (after being self-nucleated by the unmelted crystals).
- Cooling from  $T_s$ : The sample is cooled at  $10^\circ\text{C min}^{-1}$  from  $T_s$  to  $25^\circ\text{C}$ , the fraction of the polymer that was melted at  $T_s$  will crystallize during cooling, depending on the  $T_s$  applied in step (c). If the sample is in *Domain I* (or complete melting *Domain*) it will crystallize at the standard  $T_c$ , if it is in *Domain II* (or exclusive self-nucleation *Domain*) it will crystallize at a higher temperature since it will be self-nucleated, and finally, if it is in *Domain III* (or self-nucleation and annealing *Domain*) it will immediately crystallize during cooling (just below  $T_s$ ).
- Steps “c”, “d”, and “e” were repeated at progressively lower  $T_s$ . The number of repetitions (cycles) can be chosen to cover the entire melting range of the sample with a “standard” thermal history or a shorter range. For example, in the case of the HDPE samples evaluated in this research, only 7 cycles were applied (from 131 to  $101^\circ\text{C}$ ). When heating to a new  $T_s$  or fractionation step: The sample is heated once again at the same constant rate but this time to a new  $T_s$  which was  $5^\circ\text{C}$  lower than the previous  $T_s$ . The sample is held at this new  $T_s$  for 5 min. This treatment causes the unmolten crystals at this  $T_s$  to anneal and, therefore, the lamellae to thicken, some of the melted species may isothermally crystallize (after being self-nucleated by the unmelted crystals), while the rest of the molten crystallizable chain segments will only crystallize during the subsequent cooling from  $T_s$ . This step is crucial for the fractionation process, since it defines the fractionation window or temperature

- interval selected for the fractionation, i.e., in our case a  $\Delta T = 5$  °C and a fractionation time of only 5 min. The effects of changing  $\Delta T$ , time, and the initial  $T_s$  have been reviewed in the literature [17].
- (g) Final melting: The sample was heated at 10 °C min<sup>-1</sup> up to the melt state.

#### Transmission electron microscopy (TEM)

The solid state morphology was evaluated by transmission electron microscopy (TEM). The HDPE samples (original and irradiated) were prepared for TEM observation by following the next steps [24, 25]: (a) pyramidal pieces of the HDPE were obtained using an Ultracryomicrotome Reichert Jung Ultracut E.; (b) those pieces were immersed in a HCISO<sub>3</sub> solution for 24 h; (c) the pieces were washed with acetone, and ultrafine cuts (approx. 90 nm) were obtained using the ultramicrotome with a cutting rate of 1 mm/s; (d) finally, those ultrafine cuts were stained using a 2 wt% uranyl acetate ( $\text{UO}_2(\text{CH}_3\text{COO})_2 \cdot 2\text{H}_2\text{O}$ ) solution, and washed with distilled water. The stained cuts were observed with a Hitachi H-600 microscope, working at 100 kV. The experimental lamellar thickness distribution of the evaluated HDPE samples, before and after the irradiation, was determined by measuring the thickness of at least 200 lamellae on the negatives of the micrographs. Up to six micrograph negatives were analyzed by sample.

## Results and analysis

### Standard thermal properties and SSA behavior

Figure 2 shows the cooling runs from the melt of two HDPE samples before and after irradiation with 200 kGy. One very interesting feature emerges after irradiation; a rather small exotherm located at temperatures below 80 °C appears (as indicated with a circle in the cooling scan). This small endotherm is usually present in all branched PE samples (i.e., ethylene/α-olefin copolymers and low density polyethylenes) and previous studies have demonstrated that it corresponds to the intra-molecular crystallization of short linear sequences in between chain branches or in this case crosslink points [26].

The thermal properties obtained from the standard DSC runs are shown in Table 1. There it can be appreciated how the High Density Polyethylene sample irradiated with 200 kGy (HDPE200) decreased its melting peak temperature ( $T_m$ ) in approximately 3 °C in comparison to the non-irradiated original HDPE sample (from 131 to 128 °C, approx., see Fig. 3). Also, the latent heat of fusion decreased remarkably, indicating a reduction in the

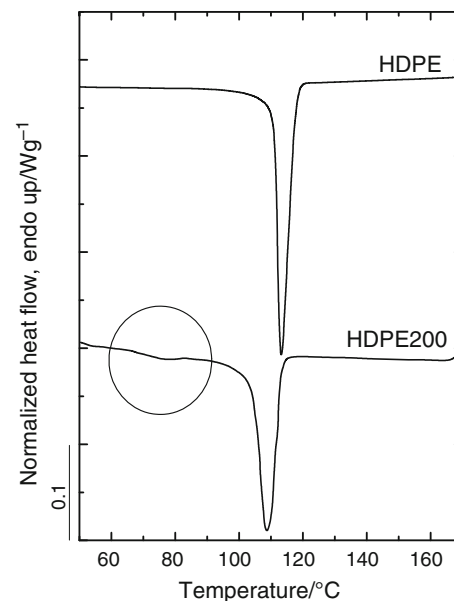


**Fig. 2** DSC cooling curves (at 10 °C min<sup>-1</sup>) for the original HDPE sample and for the sample irradiated with a 200 kGy dose (HDPE200)

**Table 1** Thermal properties of the HDPE samples evaluated

Sample	Irradiation/ kGy	$T_m$ (peak)/ °C	$T_m$ (onset)/ °C	$\Delta H_m^a$ / J g <sup>-1</sup>	$X_c^a$ / %
HDPE	—	131.3	125.8	205	71
HDPE70	70	131.0	124.1	193	67
HDPE100	100	128.9	123.9	190	69
HDPE200	200	128.1	119.5	168	58
HDPE70 <sub>GF</sub>	70	129.8	119.4	158	55
HDPE200 <sub>SF</sub>	200	129.9	124.6	250	87
HDPE200 <sub>GF</sub>	200	126.3	118.5	147	51

SF Soluble fraction, GF Gel fraction

<sup>a</sup> with a 10% error

crystallinity degree from 77 to 58%, after the exposure to the irradiation dose. These results are a consequence of the interruption of the linear crystallizable sequences within the HDPE chains produced by the irradiation process, limiting the crystallization capability of the sample and, hence, affecting the lamellar thickness (decreasing the  $T_m$  value) and the quantity of material able to crystallize (decreasing  $X_c$ ).

The irradiation of linear polyethylene will cause random crosslinking in the chains, which could be considered equivalent to the random generation of tertiary carbon atoms along the chains. The observation of the structural heterogeneities in the polyethylene chains, due to the presence of random branching in the irradiated HDPE, can be made by the application of the SSA technique, since it is highly sensitive to any interruption of the methylene sequences along the chain.

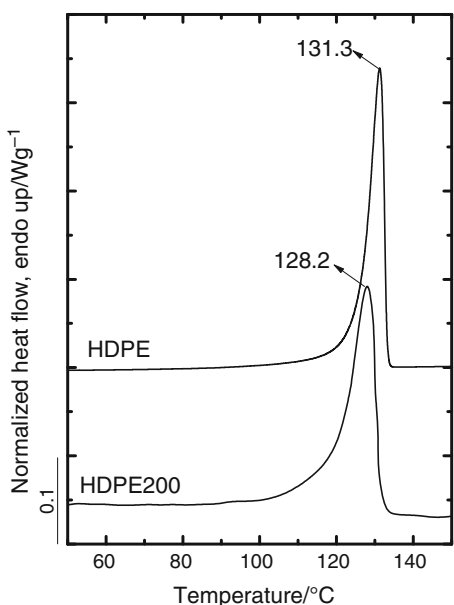


**Fig. 3** DSC heating curves ( $10\text{ }^{\circ}\text{C min}^{-1}$ ) for the original HDPE sample and for the sample irradiated with a 200 KGy dose (HDPE200)

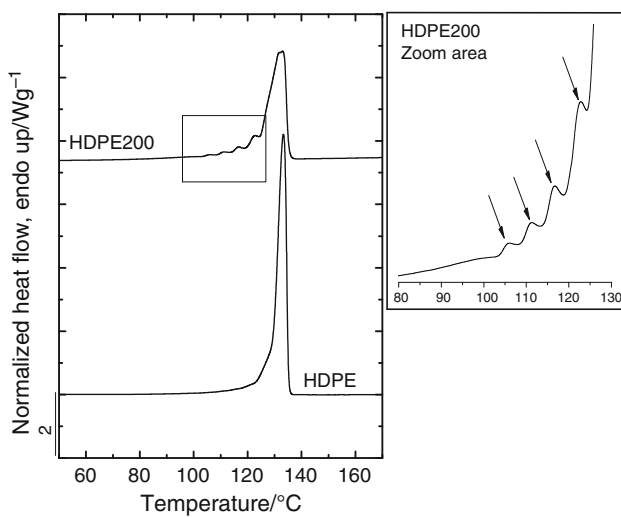


**Fig. 4** DSC final heating scan after applying SSA to the original HDPE sample and to the sample irradiated with a 200 kGy dose (HDPE200). *Inset:* zoom area of the HDPE200 curve

Figure 4 presents the final heating runs at  $10\text{ }^{\circ}\text{C min}^{-1}$  after applying the SSA thermal protocol to the original HDPE and to the irradiated HDPE200 samples. When SSA is performed to the linear HDPE, almost no fractionation was obtained, and the final heating scan (see Fig. 4) only shows one dominant single melting peak which contains a small low temperature shoulder. In the case of the HDPE200 sample, a series of discrete melting peaks can be seen, indicating that the thermal fractionation process was more successful in separating fractions for each  $T_s$  temperature employed, in view of the presence of crosslinking

points or branching points that interrupt the linear sequences within the PE chains.

According to the experimental protocol of the SSA technique applied to the HDPE samples (irradiated and non-irradiated), a total of 7 different  $T_s$  temperatures were used. The first  $T_s$  temperature of  $131\text{ }^{\circ}\text{C}$  is a temperature that should cause only self-nucleation in the polymer, according to our previous self-nucleation experiments on these samples (i.e., this  $T_s$  temperature is within Domain II [17]). Therefore, a total of 6  $T_s$  temperatures should be capable of producing annealing and thermal fractionation. Nevertheless, because we are dealing with samples with relatively low levels of methylene sequence interruptions (by chain branching or crosslinking), a maximum of only 5 melting peaks were obtained. Figure 4 shows that five melting peaks were produced after SSA in the irradiated sample; these fractions indicate that the HDPE was susceptible to modification of its linear sequences due to the irradiation dose applied. The broad fraction with the highest melting point correspond to two thermal fractions that were not separated with the fractionation conditions employed (i.e., the thermal fractions produced by the  $T_s$  temperatures of  $126$  and  $121\text{ }^{\circ}\text{C}$ , see Table 2). These two fractions grouped on the highest temperature melting peak correspond to the fusion of the thickest lamellae which are constituted by the longest uninterrupted methylene sequences in all the different chains within the polymer. SSA has the advantage of producing thermal fractions that can originate from within the same chain (intra-molecular fractionation) or from different chains (inter-molecular fractionation) within a given PE sample. In the present case, this higher melting point fraction is also the most abundant one and it is followed by the other four, less abundant fractions that appear at lower melting temperatures, as it can be seen in Fig. 4 (see the close-up).

The above-mentioned trend after SSA fractionation was observed for most of the irradiated HDPE samples (one exception being sample HDPE200<sub>GF</sub> in view of its lower melting point, see below). Upon increasing the radiation dose (from 70 to 200 KGy), the HDPE evidenced more pronounced fractionation. The peak temperatures and the height of the endotherm peaks obtained after applying the SSA thermal protocol on the irradiated HDPE are presented in Table 2. In this table it can be clearly seen how the number of fractionated endotherms increased with the radiation dose. The highest melting peak endotherm always corresponds to two thermal fractions grouped together as explained above (i.e., the two highest melting point overlapping fractions should correspond to  $T_{m_1}$  and  $T_{m_2}$  in Table 2). In the case of sample HDPE200<sub>GF</sub>, the first two  $T_s$  temperatures are wasted in the sense that they do not produce annealing since the first one is in Domain I (melting domain, i.e.,  $131\text{ }^{\circ}\text{C}$ ) and the second one in

**Table 2** Melting peak fractions obtained after applying the SSA thermal protocol to the HDPE and irradiated HDPE samples

Samples	$T_{m_1}/^{\circ}\text{C}$ ( $h_1$ )	$T_{m_2}/^{\circ}\text{C}$ ( $h_2$ )	$T_{m_3}/^{\circ}\text{C}$ ( $h_3$ )	$T_{m_4}/^{\circ}\text{C}$ ( $h_4$ )	$T_{m_5}/^{\circ}\text{C}$ ( $h_5$ )	$T_{m_6}/^{\circ}\text{C}$ ( $h_6$ )
HDPE	133.9 (65.4)	—	—	—	—	—
HDPE70	133.4 (43.3)	**	121.9 (3.74)	116.6 (1.9)	112.7 (1.0)	105.9 (0.5)
HDPE70 <sub>GF</sub>	132.4 (40.1)	**	121.8 (6.8)	116.2 (2.3)	111.1 (1.9)	105.3 (1.1)
HDPE200	130.5 (33.2)	**	121.5 (6.9)	116.1 (3.3)	111.1 (1.9)	106.0 (1.0)
HDPE200 <sub>SF</sub>	132.1 (64.5)	**	—	—	—	—
HDPE200 <sub>GF</sub>	—	128.6 (21.2)	**	117.7 (4.2)	112.3 (2.2)	107.3 (1.2)
$T_s$ temperature (°C)	126	121	116	111	106	101

$T_m$  melting peak temperature of each observed fraction,  $h$  height (in mW) of each endothermic peak

\*\* The melting peak corresponding to the second thermal fraction ( $T_{m_2}$ ) was not observed because it was always overlapped with  $T_{m_1}$ , except for HDPE200<sub>GF</sub> where  $T_{m_2}$  and  $T_{m_3}$  are overlapped

Domain II (self-nucleation Domain, i.e., 126 °C). Therefore, according to Table 2, for these samples the two fractions that overlap with one another are those corresponding to  $T_{m_2}$  and  $T_{m_3}$ .

When the HDPE samples are exposed to an irradiation dose, a number of active radicals will be originated within a fraction of the material. These active radicals will promote the formation of a crosslinked network between the HDPE highly linear chains. Hence, when the irradiated HDPE sample is solubilized, we can separate two main fractions: (i) the soluble fraction, i.e., the one formed by the uncrosslinked and still soluble HDPE chains, and (ii) the gel fraction, i.e., the reticulated HDPE fraction which turned insoluble.

Figure 5 compares the final heating runs after SSA fractionation of HDPE70 and the gel fraction extracted from this sample (i.e., HDPE70<sub>GF</sub>). In the case of the HDPE70<sub>GF</sub> sample, Fig. 5 shows that after the SSA

fractionation, this gel fraction exhibits a higher susceptibility to fractionation than HDPE70 because the thermal fractions are slightly better defined (see the zoom areas within Fig. 5). The fractionation observed for the HDPE70 is the contribution of the fractionation that could be obtained by applying SSA to both the soluble and the gel fraction of this sample. However, since the soluble fraction (formed only by non-crosslinked HDPE chains) did not fractionate at all (it gave the same result as that seen in Fig. 4 for HDPE), then the gel fraction should be the main responsible for the overall fractionation observed for the global HDPE70 sample. In fact in both the HDPE70 and the HDPE70<sub>GF</sub> samples, the fact that the main high temperature melting peak is made up of two fractions becomes evident, since after the highest melting peak a small low temperature shoulder or change in slope can be seen, although this change is more pronounced in the HDPE70<sub>GF</sub> sample (as indicated with an arrow in Fig. 5), as expected.

The percentage of quantified gel fractions is presented in Fig. 6 as a function of the radiation dose applied to the

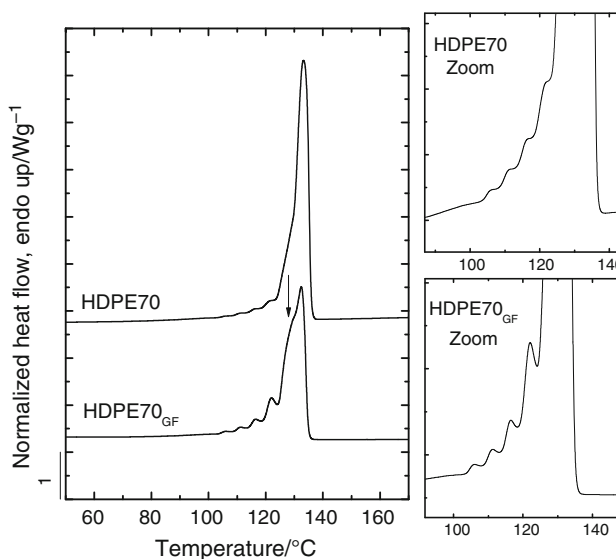


**Fig. 5** DSC final heating scan after applying SSA to the irradiated HDPE70 sample and its gel fraction (HDPE70<sub>GF</sub>). Inserts: zoom areas

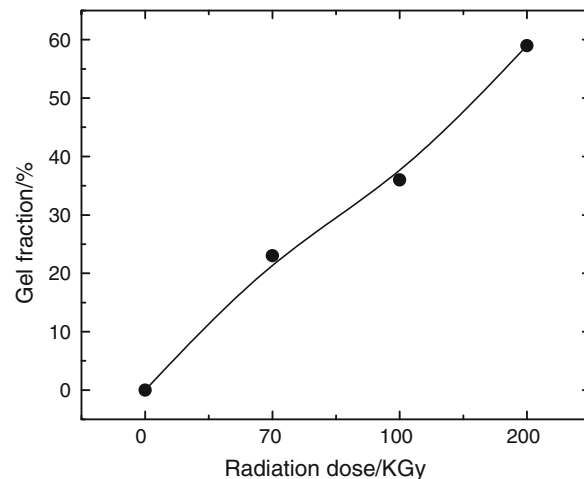


**Fig. 6** Variation of the gel fraction content as function of the radiation dose

samples. As expected, the amount of crosslinked HDPE chains (i.e., which is proportional to the gel fraction) increases significantly with the increase of the irradiation dose (to a value where the gel fraction increases above 50% at the highest irradiation dose).

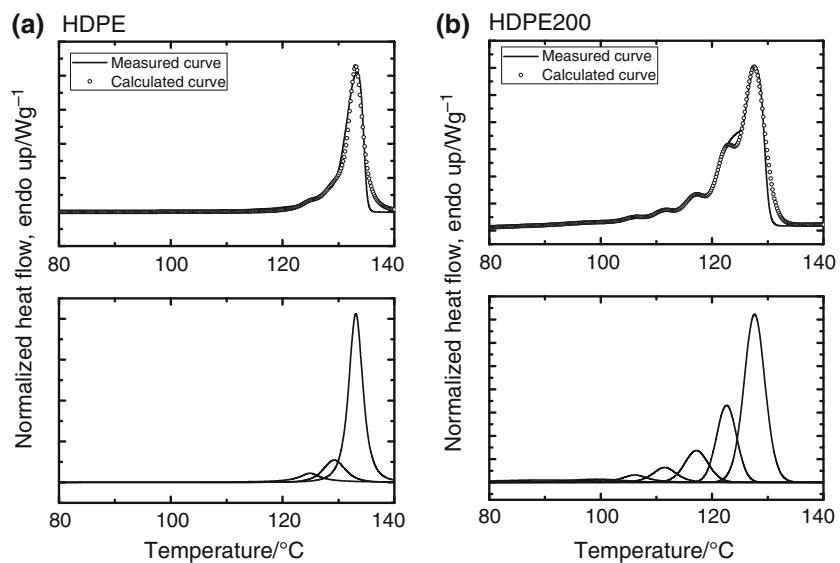
In order to make some quantitative comparisons between the results after SSA, it is useful to separate and quantify the heights and areas of each melting peak obtained after the SSA was applied, i.e., the amount of each thermal fraction. It is also desirable to have both discrete and continuous values of the amount of material contained in each melting fraction. One way to obtain discrete height and area values was suggested by Zhang and Wanke [27] and recently employed by Lorenzo et al. [18], and it consists in performing a deconvolution of the heating DSC scan into elementary curves by employing the commercial software Peakfit® (version 4.12 from SPSS Science Inc.). The function employed in this study for the deconvolution procedure was the Pearson VI area function given by the software as:

$$y = \frac{a_0 a_3 \exp \left[ a_3 \tan^{-1} \left[ \frac{T + \frac{a_2 a_3}{2} - a_1}{a_2} \right] \right]}{a_2 \left[ \exp \left( \frac{a_3 \pi}{2} \right) - \exp \left( \frac{a_1 \pi}{2} \right) \right] \left[ 1 + \frac{\left( T + \frac{a_2 a_3}{2} - a_1 \right)^2}{a_2^2} \right]} \quad (1)$$

where  $y$  is the heat flow,  $T$  is the DSC temperature,  $a_0$  is the signal amplitude,  $a_1$  is the signal center point,  $a_2$  is the peak width at half height, and  $a_3$  is a shape factor.

The individual peaks resulting from the deconvolution of the final endotherm obtained after the SSA treatment applied to the HDPE and the irradiated HDPE200 are shown at the bottom of Fig. 7 while the top shows the excellent fit obtained in comparison to experimental data. The areas and heights of each peak are part of the Peakfit® output.

**Fig. 7** Results of the fitting of DSC final heating scans after applying SSA to HDPE (left) and HDPE70 (right). Top: a comparison of measured (dotted line) and fitted (solid line) data; Bottom: deconvoluted peaks



Since the effect of crosslinking is the same as that obtained by introducing branches along the PE chain, in the sense that it is the interruption of the linear methyl sequences that produce the fractionation, then we can employ relationships that have been derived in the literature for branched polyethylenes in order to relate the thermal fractions to a specific content of branches.

The relationship between  $T_m$  and the average cross-link points (CLP), a value very similar to the short chain branching degree (SCB, i.e., number of branches per each 1000 carbons), can be calculated from the following relationship, which considers chain branches of a length comparable to six methyl units (from ethylene/1-octene copolymers) [28]:

$$T_m = -2.18 \times CLP + 134 \quad (2)$$

Using the  $T_m$  values from each melting peak found for the samples after applying the SSA thermal protocol and employing Eq. 2, we can construct Fig. 8. In this figure, the CLP parameter (a parameter which is analog to the density of crosslinking points in irradiated HDPE) increases with the amount of radiation dose until it reaches a top value of 10.2 at 200 kGy. In general, a decrease in the high temperature melting peak areas and an increase in the low temperature melting peak areas are observed as irradiation dose increases. Also, a widening of the CLP distribution is also observed (from values that encompass a range 0.1–2 for HDPE to much wider distributions encompassing a range 0.1–10.2 for HDPE200). The data reported in Fig. 8 represent a precise characterization of the irradiated polyethylenes employed here using a simple DSC-based technique such as the SSA thermal fractionation. The figure shows a quantitative distribution of chain heterogeneity induced by crosslinking and expressed as CLP content.

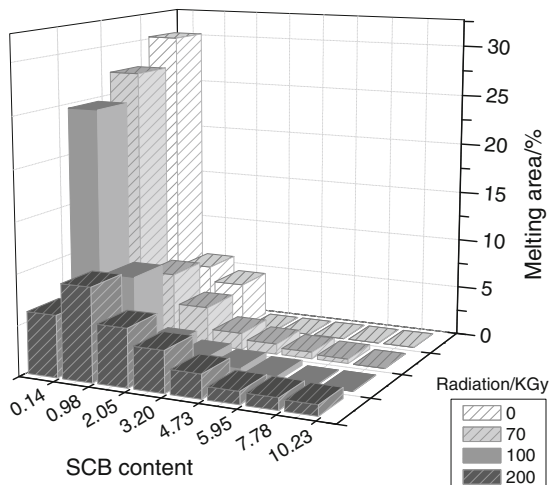


**Fig. 8** Partial area distribution of the evaluated sample, determined from the DSC final heating scan after applying SSA to using the PeakFit® program, as function of the Short Chain Branching (SCB) content and of the radiation dose

#### Transmission electron microscopy

After the HDPE and HDPE200 samples were subjected to SSA treatments, they were observed by *TEM* and their respective morphologies are shown in Fig. 9 (these micrographs were reported in a previously published extended abstract, ref. [29]). Most of the lamellae that can be observed in the HDPE sample are long and straight (as indicated by the two white arrows that follow the contour length of one lamella as an example), as expected for a highly linear polyethylene sample submitted to either a long isothermal crystallization procedure or as in this case to a fractionation protocol that drives the morphology closer to the equilibrium [30]. A striking difference is observed for HDPE200 at the same magnification. The presence of a large number of curved and much shorter lamellae (black arrows point two examples) is remarkable. This type of "C" lamellae are common in branched polyethylenes and also in crosslinked ones because they share

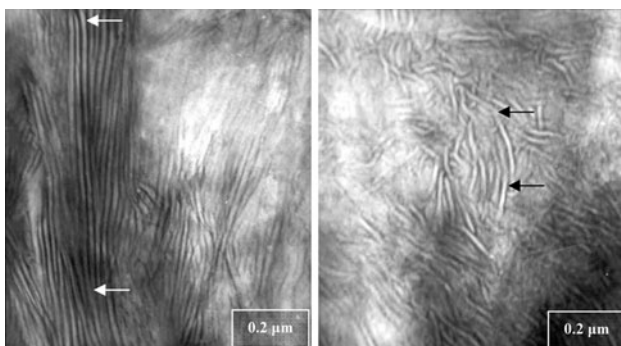


**Fig. 9** TEM micrographs for the HDPE and HDPE200 samples taken from ref [32]

the same origin: the frequent interruption of the linear sequences by tertiary carbon atoms [30]. Another salient feature which corresponds with the results of Fig. 8 obtained by SSA is that a wide distribution of lamellar thicknesses is apparent in the HDPE200 sample in comparison to the non-irradiated HDPE sample. The presence of a larger population of thicker lamellae in HDPE as compared to HDPE200 is clearly evident when the micrographs of Fig. 9 are compared. This is an expected result based on the information compiled in Fig. 8 and Table 2.

A large number of images (approximately 6 micrographs per sample) were measured in order to calculate an experimental distribution of lamellar thicknesses. An apparent lamellar thickness can be calculated theoretically by employing the Gibbs–Thomson equation [31, 32] or a modified version of this equation which has been recently introduced by Cho et al. [33]:

$$l = \frac{2\sigma T_m^0 \Delta z}{\Delta h(T_m^0 - T_m)} \quad (3)$$

where  $\sigma$  is the lamellar surface free energy,  $\Delta h$  is the enthalpy of fusion per C<sub>2</sub>H<sub>4</sub>-group (values of 5.0 and 8.2 kJ mol<sup>-1</sup> are recommended for polyethylene by Cho et al. [33]),  $\Delta z$  is the length of a C<sub>2</sub>H<sub>4</sub>-unit in chain direction (0.254 nm), and  $T_m^0$  is the equilibrium melting temperature. The above equation assumes that  $\sigma$  and  $\Delta h$  are constants as the material is being melted, and the results are highly dependent on the value of  $T_m^0$ . A  $T_m^0$  value of 145.5 °C has been employed here, even though this value would be only strictly applicable to the uncrosslinked sample. However, for comparison purposes, we employed the same value in both cases.

For the HDPE and HDPE200 samples, Table 3 and Fig. 10 present the experimental and apparent calculated lamellar thickness distributions. In this case, the modified Gibbs–Thomson equation predicts a qualitatively similar lamellar thickness distribution than the one obtained from the TEM measurements. From the obtained results it can be concluded that the modified Gibbs–Thomson equation is useful to compare apparent lamellar thickness distributions obtained by SSA, after applying the thermal fractionation

**Table 3** Comparison between experimental and theoretical (apparent) lamellar thickness distribution, for the HDPE and HDPE200 samples

Sample	<i>l/nm</i>	
	By TEM	By theory
HDPE	11.3 to 16.3	17.8
HDPE200	6.3 to 11.3	5.1 to 13.4

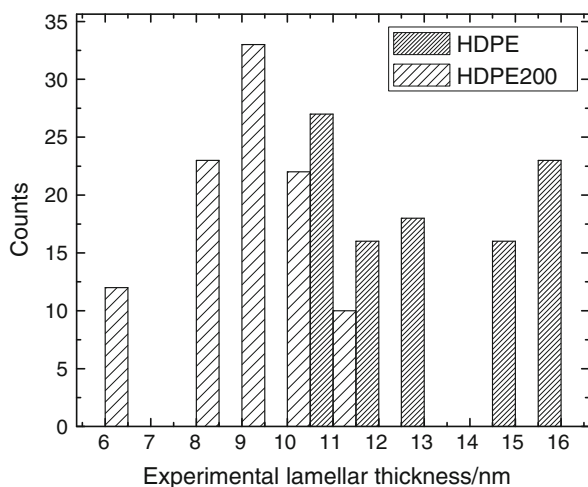


**Fig. 10** Experimental lamellar thickness histogram, obtained from the TEM micrographs, for the neat PEAD and the irradiated PEAD200 samples

to HDPE samples with different gel contents due to prior irradiation process.

## Conclusions

Successive Self-nucleation and Annealing thermal fractionation can yield valuable information of the structural changes induced in high density polyethylene by irradiation. The production of tertiary carbon atoms during the crosslinking reactions induced by irradiation can be equivalent to the structural heterogeneity present in branched polyethylenes since in both cases interruption of the linear crystallizable sequences occur, which are the structural differences that can be easily detected by thermal fractionation.

We have employed an empirical correlation between melting point and short chain branching content (adapted for CLPs) determined for branched polymers, and we have derived a distribution of chain heterogeneity produced by crosslinking. Irradiation induces random crosslinking reactions that produce a specific distribution of chain defects.

As the crosslinking degree (determined by the gel content) increases, the distribution of chain heterogeneity gets broader as determined by SSA. When the results are coupled with morphological observations made by TEM, valuable information on the morphological changes produced by crosslinking can also be ascertained, since the distribution of lamellar thicknesses substantially broadens with crosslinking. Such a broad distribution can also be predicted from simple calculations performed employing a modified version of the Gibbs–Thomson equation and is expected on the basis of random crosslinking reactions.

**Acknowledgements** This study was funded by the “Fondo Nacional de Ciencia, Tecnología e Innovación” (FONACIT) in Venezuela, through the grant F-2005000236, and by the Universidad de Oriente (IBCAUDO and Research Council). The authors are grateful to Lic. Augusto García and Dr. M. Failla (Planta Piloto de Ingeniería Química, PLAPIQUI UNS-CONICET, Argentina) for their collaboration in several aspects of this research.

## References

- Randall JC, Zoepfl FJ, Silverman J. A  $^{13}\text{C}$  NMR study of radiation-induced long-chain branching in polyethylene. *Die Makromolekulare Chemie Rapid Communications*. 1983;4:149–57.
- Vallés EM, Failla MD. The effect of temperature on the tensile mechanical behavior of irradiated linear polyethylene. *J Appl Polym Sci*. 2003;88:1925–35.
- Albano C, Perera R, Silva P, Sánchez Y. Characterization of gamma irradiated PEs using ESR FTIR and DSC techniques. *Polym Bull*. 2003;51:135–42.
- Pérez CJ, Vallés EM, Quinzani LM, Failla MD. Polyethylenes modified by irradiation and organic peroxide treatment: rheological study. *Lat Am Appl Res*. 2003;33:109–14.
- Pérez CJ, Cassano GA, Vallés EM, Failla MD, Quinzani LM. Rheological study of linear high density polyethylenes modified with organic peroxide. *Polymer*. 2002;43:2711–20.
- Perez CJ, Cassano G, Vallés EM, Quinzani LM, Failla MD. Tensile mechanical behavior of linear high-density polyethylenes modified with organic peroxide. *Polym Eng Sci*. 2003;43:1624–33.
- Perez CJ, Villarreal N, Pastor JM, Failla MD, Valles EM, Carella JM. The use of SSA fractionation to detect changes in the molecular structure of model ethylene–butene copolymers modified by peroxide crosslinking. *Polym Degrad Stabil*. 2009;94:1639–45.
- Andersson LHU, Gustafsson B, Hjertberg T. Crosslinking of bimodal polyethylene. *Polymer*. 2004;45:2577–85.
- Bremner T, Rudin A. Modification of high density polyethylene by reaction with dicumyl peroxide. *Plast Rubber Process Appl*. 1990;13:61–6.
- Márquez L, Rivero I, Müller AJ. Application of the SSA calorimetric technique to characterize LLDPE grafted with diethyl maleate. *Macromol Chem Phys*. 1999;200:330–7.
- Rojas de Gáscue B, Méndez B, Manosalva JL, López J, Ruiz Santa Quiteria V, Müller AJ. Experimental analysis of the grafting products of diethyl maleate onto linear and branched polyethylenes. *Polymer*. 2002;43:2151–9.
- Smedberg A, Hjertberg T, Gustafsson B. Crosslinking reactions in an unsaturated low density polyethylene. *Polymer*. 1997;38:4127–38.
- Smedberg A, Hjertberg T, Gustafsson B. Effect of molecular structure and topology on network formation in peroxide cross-linked polyethylene. *Polymer*. 2003;44:3395–405.
- Quero E, Puig CC, Albano C, Karam A.  $\gamma$ -Radiation (0–150 KGy) effects on slow and fast cooled HDPE/LDPE Blends. *Polym Bull*. 2007;59:517–26.
- Müller AJ, Hernández ZH, Arnal ML, Sánchez JJ. Successive self-nucleation/annealing (SSA): a novel technique to study molecular segregation during crystallization. *Polym Bull*. 1997;39:465–72.
- Arnal ML, Balsamo V, Ronca G, Sánchez A, Müller AJ, Cañizales E, Urbina de Navarro C. Applications of successive self-nucleation and annealing (SSA) to polymer characterization. *J Thermal Anal Calorim*. 2000;59:451–70.
- Müller A, Arnal ML. Thermal fractionation of polymer. *Prog Polym Sci*. 2005;30:559–603.

18. Lorenzo AT, Arnal ML, Müller AJ, Boschetti de Fierro A, Abetz V. High speed SSA thermal fractionation and limitations to the determination of lamellar sizes and their distributions. *Macromol Chem Phys.* 2006;207:39–49.
19. Müller AJ, Lorenzo AT, Arnal ML. Recent advances and applications of Successive Self-Nucleation and Annealing (SSA) high speed thermal fractionation. *Macromol Symp.* 2009;277:207–14.
20. Varga J, Menczel J, Solti A. The melting of high-pressure polyethylene subjected to stepwise heat-treatment. *J Therm Anal.* 1979;17:333–42.
21. Varga J, Menczel J, Solti A. Memory effect of low-density polyethylene crystallized in a stepwise manner. *J Therm Anal.* 1976;10:433–40.
22. Paolini Y, Ronca G, Feijoo JL, Da Silva E, Ramírez J, Müller AJ. Application of the SSA calorimetric technique to characterise an XLPE insulator aged under multiple stresses. *Macromol Chem Phys.* 2001;202:1539–47.
23. Fillon B, Wittmann JC, Lotz B, Thierry A. Self-nucleation and recrystallization of isotactic polypropylene ( $\alpha$  phase) investigated by differential scanning calorimetry. *J Polym Sci Polym Phys.* 1993;31:1383–93.
24. Kanig G. Neue elektronenmikroskopische untersuchungen über die morphologie von polyathylene. *Prog Colloid Polym Sci.* 1975;57:176–91.
25. Puig CC. The nucleation effect of linear polyethylene lamellae over the crystallization of branched polyethylene. *Polym Bull.* 1996;36:361–7.
26. Fatou JG. Morphology and crystallization in polyolefins. In: Vasile C, editor. *Handbook of polyolefins.* New York: Marcel Dekker Inc. Chapter 8;1993.
27. Zhang M, Wanke S. Quantitative determination of short-chain branching content and distribution in commercial polyethylenes by thermally fractionated differential scanning calorimetry. *Polym Eng Sci.* 2003;43:1878–88.
28. Hosoda S. Structural distribution of linear low-density polyethylenes. *Polym J.* 1988;20:383–97.
29. Prin JL, Rojas de Gascue B, García A, Hernández G, Figuera W, Vallés EM, Failla M, Müller AJ. Caracterización de la morfología lamelar en un PEAD irradiado y fraccionado térmicamente (SSA) utilizando microscopía electrónica de transmisión. *Rev Iberoam Polim.* 2008;9:322–5.
30. Bassett DC. *Principles of polymer morphology.* Cambridge: Cambridge University Press; 1981.
31. Lu L, Alamo RG, Mandelkern L. Lamellar thickness distribution in linear polyethylene and ethylene copolymers. *Macromolecules.* 1994;27:6571–6.
32. Mandelkern L. *Crystallization of polymers. Equilibrium concepts, vol. 1.* Cambridge: Cambridge University Press; 2002.
33. Cho TY, Heck B, Strobl G. Equations describing lamellar structure parameters and melting points of polyethylene-co-(butane/octane)s. *Colloid Polym Sci.* 2004;282:825–32.